Bouncing motion of spherical particles in fluids

Philippe Gondret, M. Lance, Luc Petit

Bouncing motion of spherical particles in fluids

P. Gondret[a)]
Laboratoire Fluides, Automatique et Systèmes Thermiques, Universités P. & M. Curie et Paris-Sud et CNRS (UMR 7608), Bât. 502, Campus Universitaire, F-91405 Orsay Cedex, France

M. Lance
Laboratoire de Mécanique des Fluides et d'Acoustique, Ecole Centrale de Lyon, Université Lyon I et CNRS (UMR 5509), 36, avenue de Collongue, F-69131 Ecully Cedex, France

L. Petit
Laboratoire de Physique de la Matière Condensée, Université de Nice et CNRS (UMR 6622), Parc Valrose, F-06108 Nice Cedex 2, France

(Received 1 August 2000; accepted 18 October 2001)

We investigate experimentally the bouncing motion of solid spheres onto a solid plate in an ambient fluid which is either a gas or a liquid. In particular, we measure the coefficient of restitution e as a function of the Stokes number, St, ratio of the particle inertia to the viscous forces. The coefficient e is zero at small St, increases monotonically with St above the critical value $\mathrm{St_c}$ and reaches an asymptotic value at high St corresponding to the classical ''dry'' value $e_{\max}$ measured in air or vacuum. This behavior is observed for a large range of materials and a master curve $e/e_{\max} = \mathrm{f(St)}$ is obtained. If gravity is sufficient to describe the rebound trajectory (after the collision) in a gas, this is not the case in a liquid where drag and added-mass effect are important but not sufficient: History forces are shown to be non-negligible even at large Reynolds number. © *2002 American Institute of Physics.* [DOI: 10.1063/1.1427920]

I. INTRODUCTION

The collision of particles is a subject of continued interest since many years. Most of the studies deal with dry collisions, i.e., collisions in vacuum or in a fluid of negligible resistance, and only a few studies concern the influence of the fluid on the collision process. Concerning the dry case, the studies are numerous, both experimentally and theoretically. An important parameter describing the collision is the coefficient of elastic restitution, defined as the ratio of the velocity just after the collision to the velocity just before this collision. After the theory of elastic impact of Hertz in 1880,[1] numerous studies have been made for taking into account some inelasticity, i.e., energy losses that make the coefficient of restitution being lower than one. Inelasticity may arise from various effects such as vibrations radiated in the materials, plastic deformation or viscoelasticity of the materials. The vibrations excited by the impact may be surface or bulk waves, and vibrational modes. The plasticity may be due to small plastic indentations or fully plastic deformation. All these effects lead to energy losses that increase with the impact velocity: The coefficient of restitution decreases with the impact velocity with power laws of small exponents, typically 3/10 when elastic waves are excited in a massive plane body,[2,3] 1/5 when vibrational modes are excited in a thin target,[4–6] 1/4 when fully plastic deformation occurs,[7–10] or 1/5 when viscoelastic properties are considered.[11–14] Otherwise, some recent experiments of Falcon *et al.*[15] show a decrease of the coefficient of restitution when the impact velocity decreases to very low values. They also explain this decrease with a viscoelastic model.

On the contrary, there is much less work on the influence of the fluid on the solid–solid collision. To our knowledge, the first significant study concerning that point is the theoretical one of Davis, Serayssol, and Hinch,[16] which performed elaborate numerical simulations in order to simultaneously account for the elastic deformation of the solid surfaces and fluid pressure based on lubrication approximation close to contact. In their elastohydrodynamic approach, the authors claim that the pertinent number for the collision is not the Reynolds number Re but the Stokes number $\mathrm{St} = (2/9)\rho_s UR/\mu = (1/9)(\rho_s/\rho_f)\mathrm{Re}$ which compares the particle inertia to the viscous forces (ρ_s is the particle density, $2R$ the particle diameter, μ the fluid dynamic viscosity, and U the particle velocity). For low St, the particle does not show any rebound, as the elastic energy stored by the solid deformation is finally dissipated totally in the fluid. For St larger than a critical transition value $\mathrm{St_c}$ (slightly larger than unity), the particle shows a reverse motion of bouncing, and the authors calculate the equivalent coefficient of restitution which increases from zero above the transition. Note that $\mathrm{St_c}$ depends slightly upon the elastic properties of the solid materials (sphere and wall). More recently, Lian *et al.*[17] elaborated a simpler model based upon a Hertzian-type profile for the elastic deformation of the elastic spheres, that permits an (approximate) analytical resolution of the problem and leads to results very close to the ones of Davis *et al.*[16] In order to test experimentally the bouncing transition, Barnocky and Davis[18] dropped solid particles of few millimeters on a solid

a)Author to whom correspondence should be addressed. Telephone: 33 1 69 15 80 52; Fax: 33 1 69 15 80 60. Electronic mail: gondret@fast.u-psud.fr

wall covered by a thin liquid layer (about 0.1 mm thick) and observe if the particles bounced or not. They obtained values for St_c in rather good agreement with the preceding theory but they did not measure the coefficient of restitution above the transition. Lundberg and Shen[19] investigated the dependence of the coefficient of restitution upon the viscosity for the collision of a roller (disk) attached to a pendulum with a fixed ball of different diameters (few cm) and materials (steel and Nylon) covered by a thin layer of viscous oil (about 0.1 mm thick). For roughly $6<St<2\ \ 10^3$, they showed that the restitution coefficient decreases as the fluid viscosity increases. The studies of collision for particles totally embedded in a viscous fluid are even more recent. Zhang *et al.*[20] investigated both experimentally with a high speed camera, numerically with a lattice-Boltzmann technique and theoretically with a crude mechanistic model the collision of two elastic spheres in a stagnant viscous fluid for particle Reynolds number ranging from 5 to 300. Finally, the group of Zenit and Hunt investigated with a pendulum experiment the mechanics of liquid immersed collision by means of two experimental techniques.[21,22] The collision in water of beads of few millimeters in diameter and of different materials (steel, glass, Nylon, Delrin) are recorded with a high-speed camera and with a high-frequency-response pressure transducer, which allow them to extract the coefficient of restitution. Both techniques lead to a critical Stokes number for the bouncing transition of the order of $St_c \approx 10$.

In a preliminary study we had reported first results on the transition from a regime of viscous dissipation to a regime of elastohydrodynamic bouncing.[23] In the present paper, we focus on the bouncing regime and report extensive experiments made by varying the density and the elastic properties of the solid spheres, and also the density and viscosity of the fluids (gas or liquids). The experimental set-up is presented in Sec. II, and we report in Sec. III extensive measurements for the coefficient of restitution as a function of the different parameters. In the following section (Sec. IV), we present rebound trajectories (after the collision) of particles in liquids for different density ratio and different Reynolds numbers, which show the importance of history effects besides the gravity, drag, and added-mass effects.

II. EXPERIMENTAL SET-UP

The experiments consist in recording the trajectory of a solid sphere falling under gravity in a fluid (liquid or gas) onto a solid wall. We used spherical beads of different materials and of different radius R ranging from 0.5 to 3 mm. The density ρ_s and elastic coefficients (Young's modulus E and Poisson's ratio ν) of these materials are listed in Table I. The fluids used in this experiment are air, water, silicone oils of different densities ρ_f and different viscosities μ. The physical parameters of all these fluids are listed in Table II. The container is a rectangular vessel (10 cm×10 cm×30 cm) with lateral glass walls allowing visualization. The bottom wall, where the collisions held on, is made of optical quality glass with a roughness smaller than 0.2 micrometer and a thickness $b=12$ mm. The spheres can be released by two different devices. For steel spheres, we generally used an electromagnet to maintain then release the spheres. For the other materials, the device must be different: The spheres are maintained by suction at the tip of a small tube in which a lower pressure is imposed by a micropump. The two devices allow us to release the beads at a given time just under the liquid surface (if any) in order to avoid air entrainment. No significant rotation has been observed with these devices when releasing the spheres. The sphere motion is recorded by a high speed video camera (Kodak Motion Corder 1000) at 500 images/second and with an aperture time varying between 1/2000 s and 1/10 000 s. The digital images (512×240 pixels) are analyzed by the free software NIH Image. The images are first thresholded and binarized, and the centroid of the image of the particle is then determined. All these operations lead to an error for the sphere position of the order of 0.01 mm. Due to the large size of the spheres ($R \geqslant 0.5$ mm), the surface forces (e.g., London–van der Waals attractive forces and electrical double layer repulsive ones) can be neglected during the rebound. As the particle roughness may be important in the bouncing process,[22] we have made a careful roughness analysis of our spheres with a white light interferometric method (WYMCO apparatus). We found that the roughness is in all cases smaller than 1 μm, the mean peak value being 0.3, 0.7, and 0.9 μm for a 3 mm steel, glass, and Nylon sphere, respectively.

Figures 1(a) and 2(a) are examples of recorded trajectories for the case of a Teflon ball in air (Fig. 1) and a steel bead in silicone oil (Fig. 2): The distance h of the bottom apex of the sphere to the wall is displayed as a function of time t. We compute the instantaneous velocity as the time derivative of the position $\Delta h/\Delta t$ between two successive images, and the corresponding time evolutions of the veloc-

TABLE I. Physical properties of the spheres materials: Density ρ_s, Young elastic modulus E, and Poisson's ratio ν. The measured maximal coefficient of restitution e_{max} is also indicated for "dry" (in air) collisions of a sphere of the corresponding material onto a thick glass bottom wall at moderate impact velocity U_i ($\leqslant 1$ m/s) to avoid velocity dependency due to plastic deformation.

Material	$\rho_s(10^3$ kg/m$^3)$	E $(10^9$ Pa)	ν	e_{max}
Carbide tungsten	14.97	534	0.22	0.98±0.01
Stainless steel	7.8	240	0.30	0.97±0.01
Soda glass	2.5	60	0.24	0.97±0.02
Teflon	2.15	0.4	0.46	0.80±0.02
Delrin	1.41	3	0.4	0.95±0.02
Polyurethane	1.2	0.7	0.4	0.65±0.01
Nylon	1.14	2	0.45	0.90±0.02

TABLE II. Physical properties of the fluids: Density ρ_f and dynamic viscosity μ.

Fluid	ρ $(10^3$ kg/m$^3)$	μ $(10^{-3}$ Pa·s)
Air	1.2×10^{-3}	1.85×10^{-2}
Water	1.0	1
Silicone oil RV5	0.920	5
Silicone oil RV10	0.935	10
Silicone oil RV20	0.953	20
Silicone oil RV100	0.965	100

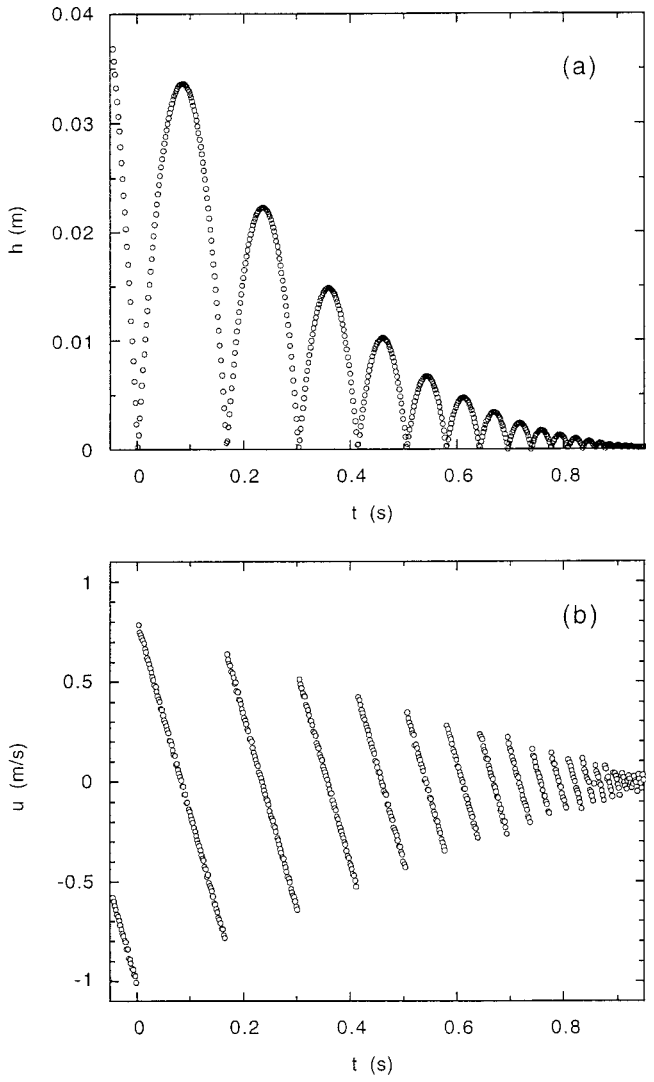

FIG. 1. Experimental (a) position h and (b) velocity u as a function of time t for a 6 mm Teflon bead impacting a glass wall in air. The Reynolds number, Stokes number and coefficient of restitution at the first impact are, respectively, Re=210, St=7.8×10^4, and $e=0.80$.

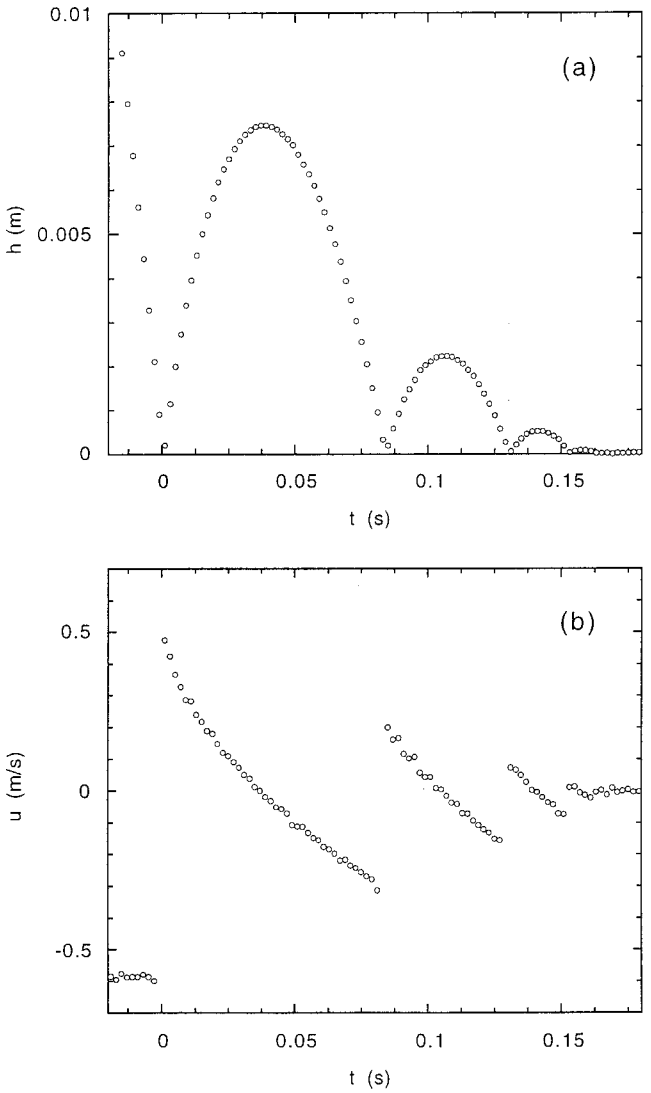

FIG. 2. Idem as Fig. 1 but for a 3 mm steel sphere in silicon oil RV10. At the first impact, Re=82, St=152, and $e=0.78$.

ity are displayed, respectively, in Figs. 1(b) and 2(b). There is here no averaging or smoothing and the error for the velocity is less than 0.01 m/s. Note that the spheres have reached generally their limit velocity before the first collision (case, e.g., of Fig. 2), except in gas (see, e.g., Fig. 1) and for the denser particles in the less viscous liquids. The coefficient of restitution e of any rebound is calculated by the ratio of the velocity U_r just after impact to the velocity U_i just before impact. For Stokes number larger than typically one, i.e., in all the bouncing regime and also just below the bouncing transition, we do not detect any decrease in the velocity before the bouncing, contrarily to what is observed in pendulum experiments.[22] This is certainly due to the fact that in our experiments gravity acts during all the pre-collision time as a motor for the sphere motion, whereas in the pendulum experiments gravity does not act anymore just before the collision with the vertical wall when the movement is horizontal. This observation allows us to determine easily if the position recorded closest to the wall corresponds to a pre- or post-collision. When colliding, the sphere decelerates and then accelerates but this occurs in a very small time: We have measured with a piezoelectric sensor that the collision duration is typically 0.01 ms, much smaller than the time between two successive images (2 ms). It is thus clear that the coefficient of restitution we measure is an effective macroscopic value. From Figs. 1 and 2, we can see that even if the coefficient of restitution for the first collision is nearly the same for the two cases (liquid or gas), the trajectories are much different. In particular, there are much less rebounds in the liquid due to the existence of fluid dissipation between the successive collisions. In the case where the ambient fluid is the air (Fig. 1), other forces than gravity are negligible: The rebound trajectories are parabolic and the velocity between collision decreases linearly with time. The velocity has the same (absolute) value at the end than at the beginning of a rebound and all the dissipation occurs during the collision. Note also that for all the successive collisions, the coefficient of restitution is nearly the same (0.80). In the other case, when the ambient fluid is a viscous liquid (Fig. 2), the

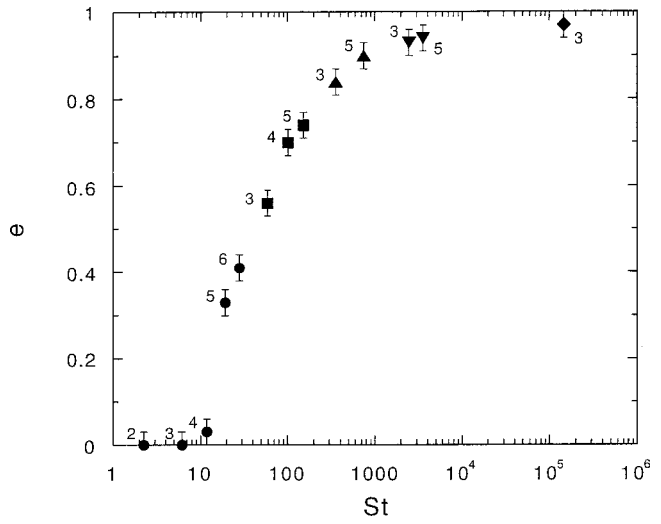

FIG. 3. Ratio e (''coefficient of restitution'') of the maximum rebound velocity u_r to the incident velocity U_i as a function of the Stokes number St. Experimental measurements for the first rebound of steel sphere of various diameters (indicated in mm beside each data point) in various fluids: Air ($\diamond$), water (∇), and silicon oils RV5 ($\triangle$), RV20 ($\square$), and RV100 ($\bigcirc$).

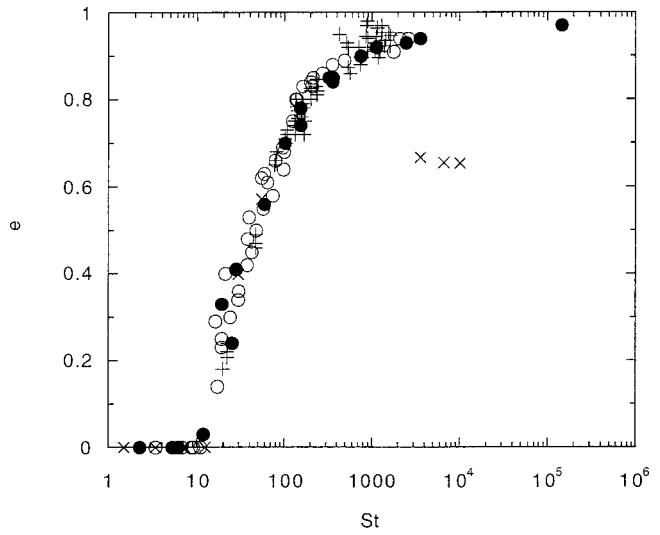

FIG. 4. Coefficient of restitution e as a function of the Stokes number St. Experimental measurements for the first rebound ($\bullet$) and following rebounds ($\bigcirc$) of steel spheres of various diameters in various fluids. Also shown are the experimental results of Gondret *et al.* (1999) ($\times$) and of Joseph *et al.* (2001) (+) corresponding to steel spheres impacting a glass or glass-like wall.

rebound trajectories are clearly non-parabolic: The velocity decreases nonlinearly with time and the velocity at the end of a rebound is significantly smaller than at the beginning. The coefficient of restitution decreases with decreasing impact velocity, being 0.78, 0.66, 0.45, 0.25, and finally 0 for the five successive collisions.

We have repeated each experiment at least three times in order to test the reproducibility of our results and estimate the dispersion. Typically, the experimental scattering for the velocity at the first impact is better than 4% in relative, and the dispersion for the restitution coefficients is better than 0.03 in absolute.

III. COEFFICIENT OF RESTITUTION

In Figs. 3–7, we present the coefficient of restitution e as a function of the Stokes number St. This choice will be justified at the end of the section where we demonstrate that the Stokes number is here the pertinent number. For a given solid material (given sphere density ρ_s), the Stokes number at impact $\mathrm{St}=(\frac{2}{9})\rho_s U_i R/\mu$ has been varied by changing the viscosity μ of the ambient fluid and the radius R of the falling spheres.

A. Coefficient of restitution of steel spheres

The evolution of the coefficient of restitution of steel spheres is displayed in Fig. 3 as a function of the Stokes number St for few fluid viscosities and particle diameters. We obtain a curve that increases monotonically for $\mathrm{St}>10$ from 0 to a value close to 1 at $\mathrm{St}\approx 10^5$. The coefficient of restitution increases abruptly just above the transition at $\mathrm{St_c}\approx 10$ and then reaches its asymptotic value (here $e_{\max}=0.97$) at large St. This $e_{\max}$ value is the classical dry value obtained for colliding spheres in fluid of negligible resistance like gas or even vacuum. The 3% dissipative part corresponds to a combined energy loss effect in the form of elastic waves, flexural vibrations of the plate and viscoelastic behavior of the bead and the target.[15] Our impact velocities at high Stokes number are small enough ($U_i \leqslant 1$ m/s) to avoid plastic deformations which make the coefficient to decrease.

B. Influence of successive rebounds

In our experiment, the particle is dropped in a initial quiescent fluid. However, the fluid is then set into motion by the successive rebounds of the particle. As a consequence, one may check if the collision is different or not for the first rebound and for the successive ones. To answer this question, we have reported in the same figure (Fig. 4) the values of the restitution coefficient for the first rebound (filled symbols) as well as for the successive ones (open symbols). Within the accuracy of our measurements, there is no difference between the two sets of measurements. One may conclude that the velocity perturbation induced by the motion of the sphere during the first rebound vanishes fast enough to have a negligible effect on the subsequent collision process, and that the collision is a very local process.

We have also reported in Fig. 4 data from other experiments[22,23] which fall reasonably on the same curve, except three points of Gondret *et al.*[23] which appear now to be very underestimated due to the previous data analysis which has been proved to be too crude for high St.

C. Wall effects

We have tested also the influence of the lateral walls and the bottom wall on the collision process. Concerning the effect of the bottom wall, it is known that the coefficient of restitution of dry impact of spheres on plates depends on the plate thickness b as flexural modes of the plates are excited for thin plates: The coefficient of restitution is a function of the ratio b/R and of the velocity U_i when the ratio b/R is small enough.[5,6] We observed this phenomenon in air as well

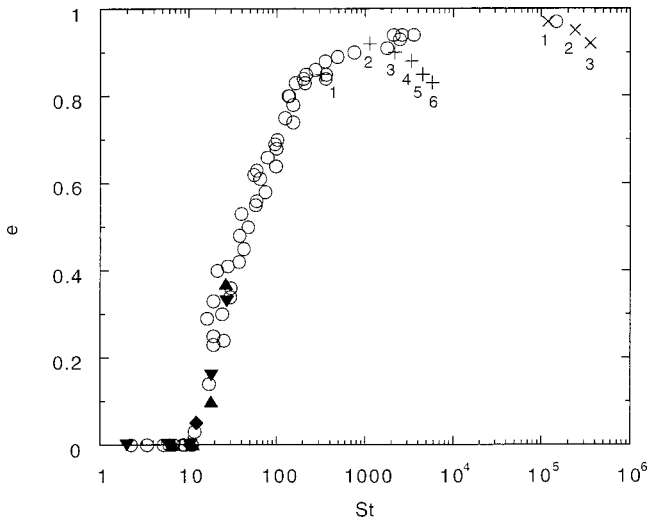

FIG. 5. Coefficient of restitution e as a function of the Stokes number St. Experimental measurements for rebounds of steel spheres of various diameters falling in various fluids contained in the entire tank of size $L=100$ mm and onto a bottom glass wall of thickness $b=12$ mm (○). Effect of lateral walls with smaller cylindrical vessels of diameter $D=40$ mm (▲), 30 mm (▼), and 12 mm (♦) (the diameters d of the falling spheres are from 4 to 6 mm). Effect of the bottom wall with a thinner plate of thickness $b=5$ mm in air (×) and water (+) (the particle diameters d are indicated here in mm beside each data point).

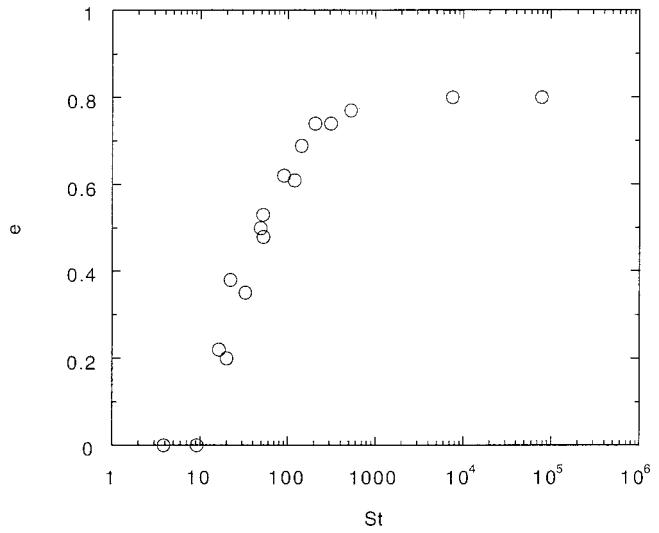

FIG. 6. Coefficient of restitution e as a function of the Stokes number St. Experimental measurements for rebounds of Teflon beads of various diameters and in various fluids.

as in water by taking a thinner bottom wall ($b=5$ mm): The restitution coefficient decreases significantly when b/R decreases (crosses in Fig. 5). With a thicker wall ($b=12$ mm), we did not observe such a phenomenon in the range of Stokes number investigated.

The influence of the lateral walls has been also investigated. At small Reynolds numbers, the long-range character of the viscous interaction is known to be responsible for the change in the terminal velocity of the sphere falling along a wall. The range of Stokes numbers of interest here corresponds to moderate and high Reynolds numbers, for which the collision process has been shown to be associated with a vortex emission.[24] In order to investigate the possible interaction of these vortices with the lateral walls and its influence on the collision, we have made several experiments at moderate Reynolds number near the bouncing transition by reducing the lateral extension of the vessel: The largest tank dimension is 10 cm while the smallest vessel diameter was 12 mm with falling spheres of diameter up to 6 mm. The results are displayed in Fig. 5 and we do not observe any effect within the accuracy of our measurements.

D. Influence of solid materials

For the measured coefficients of restitution close above the critical Stokes number, Joseph *et al.*[22] observed a dispersion that is more or less important depending on the sphere material. Making a careful study of the roughness or their spheres, they concluded that the dispersion in the results is small for smooth spheres like their steel beads and much larger for rougher particles like their glass or Nylon beads. By contrast, we did not find any significative difference in the dispersion of our results, which may be related to the fact that our plastic spheres are not much more rough than our metal spheres. Indeed, we found that the mean peak value of the roughness of a 3 mm steel, glass and Nylon sphere is 0.3, 0.7, and 0.9 μm, respectively.

For all the tested materials—tungsten carbide, glass, Delrin (polyacetal), Teflon, Nylon (polyamide) and polyurethane of different densities and elastic properties (see Table I)—we obtained a $e=\mathrm{f(St)}$ curve similar to the one already described for steel: e is zero for $\mathrm{St}<10$ and then increases with St before reaching at high Stokes the asymptotic maximum dry value $e_{\max}$ corresponding to each material (see Table I). As an example, the $e=\mathrm{f(St)}$ curve for Teflon spheres ($e_{\max}=0.80$) is displayed in Fig. 6. With our measurement precision we do not detect any significant influence of the elastic solid properties on the critical bouncing Stokes number $\mathrm{St_c}$, which is $\mathrm{St_c}\approx 10$. This observation is in agreement with the results obtained recently by Joseph *et al.*[22] with different types of spheres (glass, steel, Nylon, Delrin) and walls (glass-like and Lucite).

All these similar curves lead us naturally to plot in Fig. 7 the ratio $e/e_{\max}$ as a function of the Stokes number. All the data collapse rather well onto a single "master" curve, with a shape similar to the one predicted by the lubrication theory of Davis *et al.*[16] close to the transition even if the experimental critical Stokes number, $\mathrm{St_c}\approx 10$, is larger than the theoretical one, $\mathrm{St_c}\approx 5$, calculated for an elasticity parameter $\epsilon=10^{-5}$ corresponding to the experiments. It is worth noting that in their theoretical analysis the solid surfaces are found to not come into contact during the bouncing process. Recently, Joseph *et al.*[22] derived a simple analytical expression for an effective coefficient of restitution, by an interesting extension of the analysis of Barnocky and Davis[18] which introduces a critical distance x_c corresponding to the roughness size of the solid surfaces below which the lubrication approximation breaks down. This expression [Eq. (4.4) of

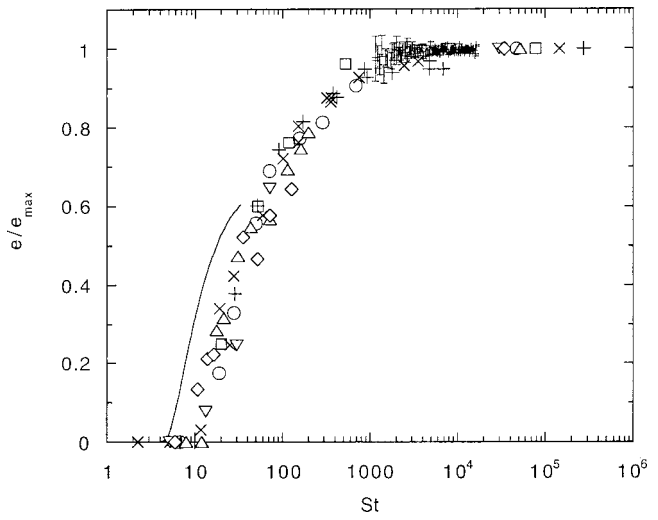

FIG. 7. Coefficient of restitution normalized by its "maximal" value $e/e_{\max}$ as a function of the Stokes number St. Experimental measurements for rebounds of beads of different materials: tungsten carbide (+), steel (×), glass (○), Teflon (□), Delrin (△), polyurethane (▽), and Nylon (◇) and lubrication theory of Davis *et al.* (1986) (——). The data of Falcon *et al.* (1998) corresponding to a bead of tungsten carbide bouncing in air are also reported with their error bars (I), by taking $e_{\max}=0.975$.

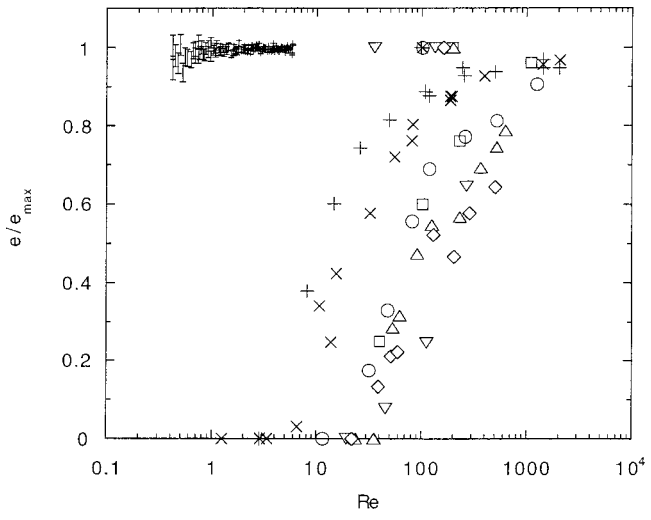

FIG. 8. Idem as Fig. 7 but as a function of the Reynolds number Re.

Ref. 22) is not compatible with our observation of a master curve $e/e_{\max}=\mathrm{f(St)}$ as it predicts that the critical Stokes $\mathrm{St_c}$ number depends on the dry value $e_{\max}$ of the coefficient of restitution, which is not the case experimentally.

Falcon *et al.*[15] have performed thorough experiments to study the behavior of the coefficient of restitution e with vanishing impact velocity U_i. To achieve this, they measured e in air for a 8 mm tungsten carbide bead impacting onto a steel pressure sensor for the last rebounds, i.e., at vanishing U_i. They found that, despite a higher scattering for the smallest rebounds, e slightly decreases when U_i approaches zero. They explained this behavior by viscoelastic effects and produced a model that predicts such a decrease. However, we wonder if this decrease may not be due to the action of air that begins to be non-negligible at these very low sphere velocities. In order to test this assumption, we have calculated the corresponding Stokes number (without taking into account a possible Maxwell slip effect that may come into play when the gap between the solid surfaces is of the order of the mean free path of the gas molecules[25]) which is found to lie between roughly 10^3 and 10^4 and we have plotted the data of Falcon *et al.* in our $e/e_{\max}=\mathrm{f(St)}$ representation. We observe that their results fall reasonably on our curve (Fig. 7), which supports the idea that the effect of ambient fluid could also explain this slight decrease. Further experiments are needed to conclude between the two explanations, for instance by reproducing these experiments in vacuum instead of air, where the ambient fluid dissipation would be negligible compared to the viscoelastic process.

Our $e/e_{\max}=\mathrm{f(St)}$ master curve shows that the Stokes number is the pertinent scaling parameter for collision processes in fluids. This is made even more clear if one looks at the evolution of the ratio $e/e_{\max}$ as a function of the Reynolds number $\mathrm{Re}=\rho_f U_i R/\mu$ based on the impact velocity U_i (Fig. 8). Figure 8 demonstrates clearly that the Reynolds number is not the pertinent parameter. The data are here highly dispersed, due to the large range of ratio ρ_s/ρ_f, changed either by varying the sphere density (roughly from 1 to 15) or the fluid density (roughly from 10^{-3} to 1). It is striking to note that the dry values measured by Falcon *et al.* correspond to Reynolds numbers ranging from 0.4 to 6. Despite these small Reynolds numbers, fluid dissipation is weak during the collision as the Stokes number is high (10^3-10^4).

In our experiments we observe some non rectilinear trajectories at the beginning of the falling of light spheres (glass and plastic materials) in water, typically for Reynolds number ranging from 2×10^2 to 2×10^3, the precise range depending on the sphere density. We have not observed this effect for the denser particles (steel and tungsten carbide) and have not been really annoyed by this effect for the determination of the coefficient of restitution.

IV. BOUNCING TRAJECTORIES

In this section, we present and discuss some preliminary results about the rebound trajectories of the spheres. In the gas case where density and viscosity of the ambient fluid are negligible, the rebound is parabolic since the gravity is the dominant force acting on the sphere (Fig. 1). In the case of a dense and viscous fluid (Fig. 2), several other non-negligible forces must be taken into account: The drag force, the force arising from the added-mass effect and the history effect. As the undisturbed ambient fluid is at rest, the equation of motion of the particle may be written as

$$\frac{4}{3}\pi R^3 \rho_s \frac{d\mathbf{U}(t)}{dt}=\mathbf{F}_g+\mathbf{F}_d(t)+\mathbf{F}_{am}(t)+\mathbf{F}_h(t). \tag{1}$$

The first term of the right-hand side of Eq. (1) is the constant gravity force $\mathbf{F}_g=\frac{4}{3}\pi R^3(\rho_s-\rho_f)\mathbf{g}$, where $\mathbf{g}$ is the gravity acceleration. The second term is the instantaneous pseudo-steady drag force $\mathbf{F}_d(t)$ that the sphere would experience in a steady motion of velocity $\mathbf{U}(t)$. It corresponds to the steady Stokes law $\mathbf{F}_d=-6\pi\mu R\mathbf{U}$ at zero Reynolds number, and deviates from this law for larger Reynolds number but may be expressed as $\mathbf{F}_d=-6\pi\mu R\mathbf{U}\phi$, where the factor

ϕ is a function of the Reynolds number Re. Many empirical expressions exist taking into account the experimental variations of $\phi(\mathrm{Re})$.[26] We will take $\phi=1+0.15\mathrm{Re}_D^{0.687}$, which is a law commonly used for Reynolds numbers Re_D (here based on the particle diameter) up to 10^3 and which compares to experimental values within a deviation of $\pm 5\%$.[26] The third term in (1) is the added-mass force which is found to be $\mathbf{F}_{am}(t)=-\frac{4}{3}\pi R^3\frac{1}{2}\rho_f[d\mathbf{U}(t)/dt]$ in the two limit cases of creeping and inviscid flows.[27] Recent numerical studies show that the added-mass term for finite-Reynolds-number flows is the same as predicted by creeping flow and potential flow theory over a wide range of the dimensionless relative acceleration.[28] Note that in the inviscid limit, this force is modified by the presence of a solid wall by the factor $(1+\frac{3}{8}R/(R+h))$, where h is the distance between the bottom of the particle and the wall.[27] This modification is not so large since this factor never exceeds 11/8. As we do not see any effect on the trajectory before the collision, we will neglect this factor in the following and thus assume that the added-mass force is given by $\mathbf{F}_{am}(t)=-\frac{4}{3}\pi R^3\frac{1}{2}\rho_f[d\mathbf{U}(t)/dt]$. The last term in Eq. (1) is the history force which may be expressed as $\mathbf{F}_h(t)=-6\pi\mu R\int_{-\infty}^{t}K(t,s;\mathrm{Re}_D)\dot{\mathbf{U}}(s)ds$, where it appears as a convolution product of the acceleration of the particle with the kernel $K(t,s;\mathrm{Re}_D)$. At zero Reynolds number the history term is known as the Basset force with the kernel $K(t,s)=[\rho_f R^2/\pi\mu(t-s)]^{1/2}$. At nonzero Reynolds number, the kernel expression for the history force is still controversial. The expression of Odar and Hamilton[29,30] modifying the Basset force just by a numerical coefficient to account for the inertial effect has been shown to be incorrect.[31] More recently, Mei and Adrian[31] proposed an approximation, based on numerical results for small oscillations about a mean flow, with a combination of two terms with different scalings. If the $t^{-1/2}$ fading effect for small times was shown to be asymptotically correct, the t^{-2} decay at long times appears to be an artifact of the interpolation procedure.[32] The analysis of Lawrence and Mei[32] and of Lovalenti and Brady[33] have shown that the asymptotic behavior of the kernel at long times may be t^{-2} or t^{-1} or even exponential, depending on the type of motion (sudden stop, sudden increase, reverse motion, . . .). To show this, they take into account the modification of the wake of the particle due to the modification of the motion. In the particular case of a reverse motion, with a constant velocity $U_r=-eU_i$ imposed after an initial constant velocity U_i, the ''old'' wake will be upstream of the particle, and will be swept back towards the body, leading thus to a lower decrease of the history force. As a matter of fact, the flow velocity near the body is increased, owing to the flux in the old wake, by an amount which scales with $1/t$ at long times. By this kind of analysis, Lawrence and Mei[32] obtained the following expression for the history force at long times: $\mathbf{F}_h(t)=-6\pi\mu R\mathbf{U}_r\phi_h(t)$, where $\phi_h(t)\sim\frac{3}{2}(\phi_r+\mathrm{Re}_{Dr}\phi_r')/(1+e)\phi_i t^{-1}$ ($\phi_{i,r}$ stands for $\phi(\mathrm{Re}_{Di,r})$ and ϕ' is the derivative of ϕ with respect to Re_D). We have chosen to take this history form in our calculations for rebound trajectories, with a numerical prefactor α as a fitting parameter.

In the following, we have focused on the first rebound trajectory. The case of a steel sphere is displayed in Fig. 9 for approximately the same incident Reynolds number ($\mathrm{Re}\approx 10^2$) in a gas (a) and in a liquid (b). Together with the experimental results (○) are shown the trajectories calculated in the case where only the gravity is taken into account (···), or with the addition of the drag force (– – –), of the added-mass effect (—·—), and finally of the history term (—). The initial rebound velocity for the calculations is the experimental one and thus not a fitting parameter. In the case where the ambient fluid is a gas [Fig. 9(a)], all the forces except the gravity are negligible and, as expected, the rebound is parabolic. In the case where the ambient fluid is a liquid [Fig. 9(b)] this is no longer true, and taking only the gravity into account leads to a large overestimate of the rebound. The dissipating role of the drag force is important to explain the smaller rebound but not sufficient, and the added-mass effect turns out to be non-negligible even for a density ratio of about 8. However, the addition of these terms is not sufficient to reproduce the experimental curve, which clearly

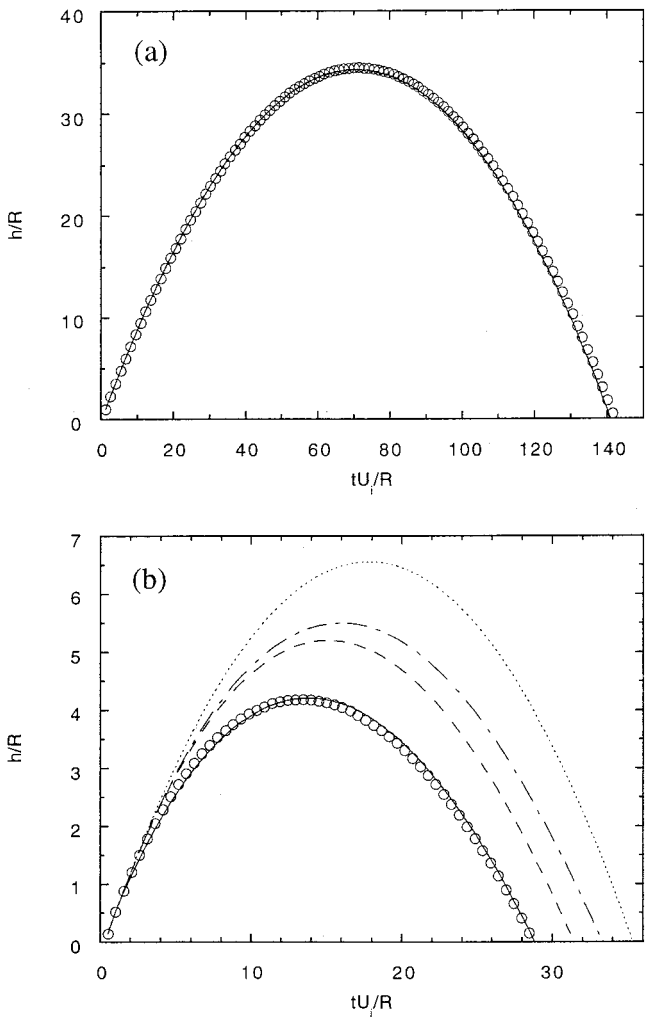

FIG. 9. Rebound trajectories for steel spheres at $\mathrm{Re}\approx 10^2$ (a) in a gas (3 mm sphere in air at Re=100) and (b) in a liquid (6 mm sphere in a silicone oil RV20, Re=106). Experimental measurements (○) and theoretical predictions taking into account F_g (---), F_g+F_d (– – –), $F_g+F_d+F_{am}$ (—·—), $F_g+F_d+F_{am}+F_h$ (—).

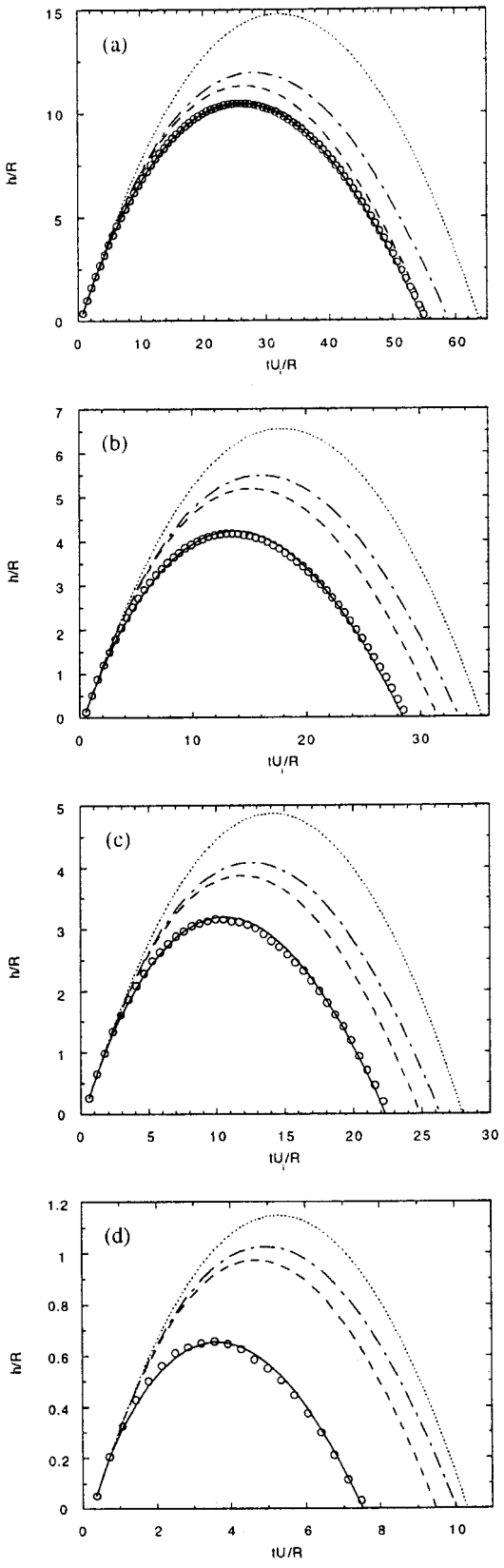

FIG. 10. Rebound trajectories for steel spheres in liquids ($\rho_s/\rho_f \approx 8$) at different Reynolds numbers: (a) Re=394 (5 mm in silicon oil RV5); (b) Re=106 (6 mm sphere in silicon oil RV20); (c) Re=55 (4 mm sphere in silicon oil RV20); (d) Re=15 (6 mm sphere in silicone oil RV100). Experimental measurements (○) and theoretical predictions taking into account F_g (---), F_g+F_d (— — —), $F_g+F_d+F_{am}$ (—·—), $F_g+F_d+F_{am}+F_h$ (—).

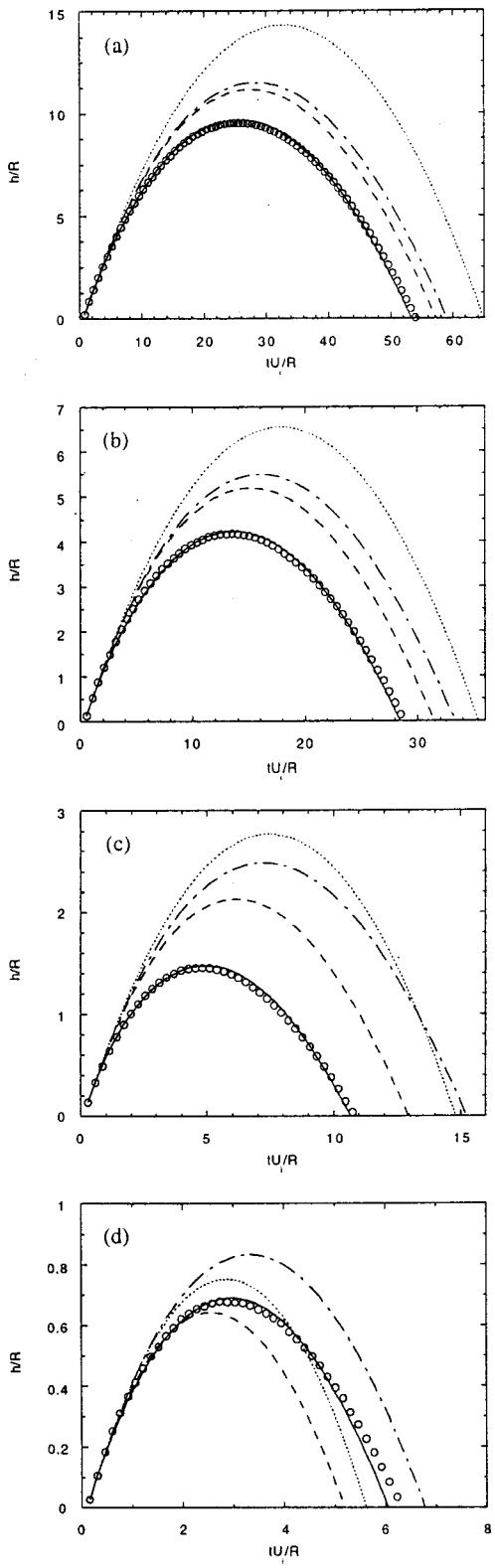

FIG. 11. Rebound trajectories for spheres of different densities in liquids at nearly the same Reynolds numbers Re$\approx 10^2$: (a) $\rho_s/\rho_f=15.7$ (5 mm tungsten carbide sphere in silicone oil RV20, Re=108); (b) $\rho_s/\rho_f=8.2$ (6 mm steel sphere in silicon oil RV20, Re=106); (c) $\rho_s/\rho_f=2.7$ (6 mm glass sphere in silicone oil RV10, Re=119); (d) $\rho_s/\rho_f=1.5$ (5 mm Delrin sphere in silicon oil RV5, Re=91). Experimental measurements (○) and theoretical predictions taking into account F_g (---), F_g+F_d (— — —), $F_g+F_d+F_{am}$ (—·—), $F_g+F_d+F_{am}+F_h$ (—).

shows that the history force is necessary to predict correctly the rebound trajectory of a sphere in a liquid.

In Fig. 10, we have shown rebound trajectories for different Reynolds numbers from 15 to 400 keeping the density ratio constant around 8 (steel spheres in different liquids). The apex of the experimental trajectories are much lower than the ones simulated with gravity alone, especially for lower Reynolds number. For increasing Reynolds number, the drag force increases while the added-mass effect is the same since the density ratio is kept constant. Therefore, the history effect turns out to be larger when the Reynolds number is lower. Note that the prefactor α in front of the history term depends slightly on the Reynolds number for a good fit, decreasing monotonically from 0.26 for $\mathrm{Re}=15$ to 0.06 for $\mathrm{Re}=394$.

In Fig. 11, we have plotted different rebound trajectories at approximately the same Reynolds number ($\mathrm{Re}\approx 10^2$) for different density ratio from 1.5 to 15. The added-mass effect that pushes up the particle after the collision is clearly enhanced when the density ratio is lower. For the lowest density ratio (1.5), this pushing effect is higher than the drag effect so that the trajectory simulated by taking into account gravity, drag and added-mass lies above the one simulated with gravity alone. In all cases, the history effect appears again necessary to predict the correct trajectory. Note that the fitting coefficient α does not depend on the density ratio, with a value around 0.1 at $\mathrm{Re}\approx 10^2$.

In all Figs. 9–11, the curve fits of the experimental trajectories with the history term are correct but not perfect. One reason may be that we neglect the wall effect in our analysis. However, we believe that this effect is weak. Another reason may be that the rebound motion is a reverse motion at a non constant velocity (the velocity decreases with time in the first part of the rebound) contrarily to the analysis of Lawrence and Mei.[32] As a consequence, the time dependence of the history term may be different.

V. CONCLUSION

In this paper, we produce extensive measurements of the apparent coefficient of restitution for the collision in fluids (gas or liquids) of solid spheres onto a solid wall. The pertinent number that characterizes the immersed collision regimes is the Stokes number which measures the particle inertia relative to the viscous forces. For low Stokes number, below the critical value $\mathrm{St_c}\approx 10$, all the particle energy is dissipated in the fluid during the collision process. In this regime, no rebound is observed and the coefficient of restitution is zero. For larger Stokes number, $\mathrm{St}>\mathrm{St_c}$, the coefficient of restitution e depends on the Stokes number St, increasing from 0 at $\mathrm{St_c}\approx 10$ towards its maximal dry value $e_{\max}$ at large St. The value of the critical Stokes number $\mathrm{St_c}$ seems surprisingly to be constant, independent of the elastic properties of the solid spheres. A master curve $e/e_{\max}=\mathrm{f(St)}$ is obtained that may be useful in the modeling of the collision process of solid particles in gas or liquid incorporated in the numerical simulations of many two-phase flows such as fluidized beds. Furthermore, we have demonstrated that history forces cannot be neglected for the bouncing trajectories after the collisions for Reynolds numbers up to about 10^3.

ACKNOWLEDGMENTS

We are grateful to Roberto Vargiolu (Laboratoire de Tribologie et Dynamique des Systèmes de l'Ecole Centrale de Lyon) for making the roughness analysis of our spheres. We acknowledge E. Falcon for providing us his data and to R. Zenit for sending us his papers. We thank N. Mordant and J.-F. Pinton for fruitful discussions.

[1] A. E. H. Love, *A Treatise on the Mathematical Theory of Elasticity* (Dover, New York, 1927).
[2] S. C. Hunter, "Energy absorbed by elastic waves during impact," J. Mech. Phys. Solids **5**, 162 (1957).
[3] J. Reed, "Energy losses due to elastic waves propagation during an elastic impact," J. Phys. D **18**, 2329 (1985).
[4] C. V. Raman, Phys. Rev. **15**, 277 (1920).
[5] C. Zener, "The intrinsic inelasticity of large plates," Phys. Rev. **59**, 669 (1941).
[6] R. Songergaard, K. Chaney, and C. E. Brennen, "Measurements of solid spheres bouncing off flat plates," ASME Trans. J. Appl. Mech. **57**, 694 (1990).
[7] C. V. Raman, "The photographic study of impact at minimal velocities," Phys. Rev. **12**, 442 (1918).
[8] K. L. Johnson, *Contact Mechanics* (Cambridge University Press, Cambridge, 1985).
[9] D. Tabor, "A simple theory of static and dynamic hardness," Proc. R. Soc. London, Ser. A **192**, 593 (1948).
[10] W. Goldsmith, *Impact* (Arnold, London, 1960).
[11] F. G. Bridges, A. Hatzes, and D. N. C. Lin, "Structure, stability, and evolution of Saturn's rings," Nature (London) **309**, 333 (1984).
[12] A. P. Hatzes, F. G. Bridges, and D. N. C. Lin, "Collisional properties of ice spheres at low impact velocities," Mon. Not. R. Astron. Soc. **231**, 1091 (1988).
[13] G. Kuwabara and K. Kono, "Restitution coefficient in a collision between two spheres," Jpn. J. Appl. Phys., Part 1 **26**, 1230 (1987).
[14] R. Ramirez, T. Pöschel, N. Brillantov, and T. Schwager, "Coefficient of restitution of colliding viscoelastic spheres," Phys. Rev. E **60**, 4465 (1999).
[15] E. Falcon, C. Laroche, S. Fauve, and C. Coste, "Behavior of one inelastic ball bouncing repeatedly off the ground," Eur. Phys. J. B **3**, 45 (1998).
[16] R. H. Davis, J.-M. Serayssol, and E. J. Hinch, "The elastohydrodynamic collision of two spheres," J. Fluid Mech. **163**, 479 (1986).
[17] G. Lian, M. J. Adams, and C. Thornton, "Elastohydrodynamic collision of solid spheres," J. Fluid Mech. **311**, 141 (1996).
[18] G. Barnoky and R. H. Davis, "Elastohydrodynamic collision and rebound of spheres: Experimental verification," Phys. Fluids **31**, 1324 (1988).
[19] J. Lundberg and H. H. Shen, "Collisional restitution dependence on viscosity," J. Eng. Mech. **118**, 979 (1992).
[20] J. Zhang, L.-S. Fan, C. Zhu, R. Pfeffer, and D. Qi, "Dynamic behavior of collision of elastic spheres in viscous fluids," Powder Technol. **106**, 98 (1999).
[21] R. Zenit and M. L. Hunt, "Mechanics of immersed particle collisions," J. Fluids Eng. **121**, 179 (1999).
[22] G. G. Joseph, R. Zenit, M. L. Hunt, and A. M. Rosenwinkel, "Particle-wall collisions in a viscous fluid," J. Fluid Mech. **433**, 329 (2001).
[23] P. Gondret, E. Hallouin, M. Lance, and L. Petit, "Experiments on the motion of a solid sphere toward a wall: From viscous dissipation to elastohydrodynamic bouncing," Phys. Fluids **11**, 2803 (1999).
[24] I. Eames and S. B. Dalziel, "Dust resuspension by the flow around an impacting sphere," J. Fluid Mech. **403**, 305 (2000).
[25] G. Barnocky and R. H. Davis, "The effect of Maxwell slip on the aerodynamic collision and rebound of spherical particles," J. Colloid Interface Sci. **121**, 226 (1988).
[26] R. Clift, J. R. Grace, and M. E. Weber, *Bubbles, Drops, and Particles* (Academic, New York, 1978).
[27] L. M. Millne-Thomson, *Theoretical Hydrodynamics* (MacMillan Education, London, 1968).

[28]I. Kim, S. Elghobashi, and W. A. Sirignano, ''On the equation for spherical-particle motion effects of Reynolds and acceleration numbers,'' J. Fluid Mech. **367**, 221 (1998).
[29]F. Odar and W. S. Hamilton, ''Forces on a sphere accelerating in a viscous fluid,'' J. Fluid Mech. **18**, 302 (1964).
[30]F. Odar, ''Verification of the proposed equation for calculation of the forces on a sphere accelerating in a viscous fluid,'' J. Fluid Mech. **25**, 591 (1966).
[31]R. Mei and R. J. Adrian, ''Flow past a sphere with an oscillation in the free-stream velocity and unsteady drag at finite Reynolds number,'' J. Fluid Mech. **237**, 323 (1992).
[32]C. J. Lawrence and R. Mei, ''Long-time behaviour of the drag on a body in impulsive motion,'' J. Fluid Mech. **283**, 307 (1995).
[33]P. M. Lovalenti and J. F. Brady, ''The temporal behavior of the hydrodynamic force on a body in response to an abrupt change in velocity at small but finite Reynolds number,'' J. Fluid Mech. **293**, 35 (1995).